© 2017. Published by The Company of Biologists Ltd | Journal of Cell Science (2017) 130, 1239-1250 doi:10.1242/jcs.197566

RESEARCH ARTICLE

Non-coding Y RNAs associate with early replicating euchromatin in concordance with the origin recognition complex

Eyemen Kheir* and Torsten Krude‡

ABSTRACT

Non-coding Y RNAs are essential for the initiation of chromosomal DNA replication in vertebrates, yet their association with chromatin during the cell cycle is not characterised. Here, we quantify human Y RNA levels in soluble and chromatin-associated intracellular fractions and investigate, topographically, their dynamic association with chromatin during the cell cycle. We find that, on average, about a million Y RNA molecules are present in the soluble fraction of a proliferating cell, and 5–10-fold less are in association with chromatin. These levels decrease substantially during quiescence. No significant differences are apparent between cancer and non-cancer cell lines. Y RNAs associate with euchromatin throughout the cell cycle. Their levels are 2–4-fold higher in S phase than in G1 phase or mitosis. Y RNAs are not detectable at active DNA replication foci, and re-associate with replicated euchromatin during mid and late S phase. The dynamics and sites of Y1 RNA association with chromatin are in concordance with those of the origin recognition complex (ORC). Our data therefore suggest a functional role of Y RNAs in a common pathway with ORC.

KEY WORDS: Non-coding Y RNA, DNA replication, Origin recognition complex, ORC, Initiation, Chromatin association, Cell cycle

INTRODUCTION

Y RNAs are abundant small non-coding RNAs in vertebrates (Hall et al., 2013; Kowalski and Krude, 2015). In human cells, four single-copy genes are transcribed by RNA polymerase III into the Y1, Y3, Y4 and Y5 RNAs of 112, 101, 93 and 83 nucleotides, respectively (Hendrick et al., 1981; Wolin and Steitz, 1983). The 5′ and 3′ RNA ends hybridise to form a double-stranded stem domain that encompasses an internal single-stranded loop domain (Teunissen et al., 2000; van Gelder et al., 1994). Nucleotide sequences of the stem are highly conserved, but those of the loop vary considerably. The structurally related stem-bulge RNAs (sbRNAs) in nematodes are homologues of vertebrate Y RNAs (Boria et al., 2010; Kowalski et al., 2015).

Y RNAs have a functional role in the replication of chromosomal DNA in vertebrate cells (Christov et al., 2006, 2008; Collart et al., 2011; Gardiner et al., 2009; Kowalski and Krude, 2015; Krude et al., 2009). They were identified as being essential for the initiation of chromosomal DNA replication in a human cell-free system (Christov et al., 2006; Krude et al., 2009). Degradation of Y RNAs *in vitro* inhibits the initiation step of chromosomal DNA replication in cell-free extracts, and RNA interference or functional depletion *in vivo* inhibits DNA replication and cell proliferation in vertebrate cells and causes death in developing vertebrate embryos (Christov et al., 2006, 2008; Collart et al., 2011). DNA replication is restored by the addition of any human or vertebrate Y RNAs to Y RNA-depleted cell-free extracts *in vitro*, or to vertebrate cells following RNA interference *in vivo*. In contrast, addition of ribosomal 5S rRNA or spliceosomal U2 small nuclear RNA (snRNA) has no effect (Christov et al., 2006; Collart et al., 2011; Gardiner et al., 2009). Therefore, vertebrate Y RNAs are required specifically for DNA replication, and they function redundantly with each other. This functional redundancy arises from the presence of an evolutionarily conserved structural motif present on the upper stem of vertebrate Y RNAs that is essential and sufficient for DNA replication (Gardiner et al., 2009; Wang et al., 2014). Consistent with a functional role in DNA replication and cell proliferation, Y RNAs are overexpressed in human solid tumour tissues, when compared with corresponding healthy normal tissues (Christov et al., 2008).

Vertebrate DNA replication is regulated during the cell cycle by the stepwise assembly and subsequent activation of multisubunit protein complexes at replication origins (reviewed by Arias and Walter, 2007; Costa et al., 2013; Fragkos et al., 2015; O'Donnell et al., 2013; Siddiqui et al., 2013). During G1 phase, the chromatin-associated origin recognition complex (ORC) directs the assembly of the pre-replication complex (pre-RC, or replication licence) at replication origin sites, involving the recruitment of Cdt1, Cdc6 and the complex of the six MCM subunits MCM2, 3, 4, 5, 6 and 7 (MCM2-7) to chromatin. During S phase, pre-RCs are converted into initiation complexes (ICs) at activated origin sites and eventually to replication fork complexes. This activation cascade involves cyclin-dependent kinase (CDK) and Dbf4-dependent kinase (DDK) protein activities and the recruitment of additional proteins, including the complex between Sld5, Psf1, Psf2 and Psf3 (also known as go-ichi-ni-san, GINS), Cdc45, DNA polymerases and many others. Crucially, after executing their function, essential subunits dissociate from the respective pre-RC, IC and replication fork complexes again, while key subunits of ORC remain associated with chromatin during the cell cycle. This process is conserved in eukaryotes.

The molecular mechanism of Y RNA function during DNA replication is not clear, although key features are emerging. Y RNAs interact biochemically with ORC, preRC components and other DNA replication initiation proteins, but not with DNA replication fork proteins (Collart et al., 2011; Zhang et al., 2011). During early development of *Xenopus laevis*, Y RNA binds to chromatin after the mid-blastula stage in an ORC-dependent manner (Collart et al., 2011). During the G1 to S phase transition *in vitro,* fluorescently labelled human Y RNAs associate dynamically with unreplicated chromatin before initiation, where they colocalise with ORC, and the preRC and IC proteins Cdt1, MCM2 and Cdc45 (Zhang et al.,

Department of Zoology, University of Cambridge, Downing Street, Cambridge CB2 3EJ, UK.
*Present address: Center for Integrative Biology (CIBIO), University of Trento, Via Sommarive 9, Povo, Trento I-38123, Italy.

‡Author for correspondence (tk218@cam.ac.uk)

T.K., 0000-0002-1842-1933

Received 19 September 2016; Accepted 13 February 2017

Journal of Cell Science (2017) 130, 1239-1250 doi:10.1242/jcs.197566

2011). Once DNA replication initiates in a Y RNA-dependent manner, Y RNAs are displaced locally and are absent from sites of ongoing DNA synthesis, suggesting they might act as DNA replication licensing factors (Zhang et al., 2011). However, Y RNAs are abundant molecules, and a comprehensive and quantitative investigation of the intracellular localisation of Y RNAs during the cell cycle has not been reported to date.

In this paper, we report the quantification of human Y RNAs in the soluble and chromatin-associated intracellular fractions of a panel of human cells. We investigate their dynamic association with chromatin during the cell cycle, and in quiescence. Using complementary approaches, we show that Y RNAs levels correlate with the proliferative state of human cells and that they associate preferentially with S phase chromatin. The dynamics of Y RNA association with chromatin throughout the cell cycle closely follow those of the ORC rather than MCM or other licensing factors, suggesting that Y RNAs act in a common pathway with ORC.

RESULTS

Quantification of Y RNAs in proliferating human cancer and non-cancer cell lines

We quantified amounts of intracellular Y RNA molecules in 12 human cell lines of cancer and non-cancer origin (Fig. 1; Table S1). Cells were grown as proliferating cultures, and then fractionated into soluble and chromatin-associated cellular compartments. After RNA extraction and cDNA synthesis, we quantified Y RNAs in these fractions by quantitative real-time RT-PCR (qPCR) using Y RNA-specific primer pairs (Christov et al., 2006). To obtain absolute numbers of Y RNA molecules per cell for each intracellular fraction, we normalised the qPCR data against defined amounts of Y RNA-specific calibrator plasmids and against the number of cells used for RNA extraction (Fig. 1).

Overall, we detected an average of a million soluble Y RNA molecules per cell (Fig. 1A). Y3 RNA was most abundant, followed by Y1, Y5 and Y4. However, this value varied between cell lines by up to an order of magnitude. There was no significant difference in soluble Y RNA levels between cancer and non-cancer derived cell lines.

In the chromatin-associated fraction, we detected an average of 150,000 Y RNA molecules per cell (Fig. 1B). Y1 and Y3 RNAs were most abundant, followed by Y5 and Y4. Again, there was no significant difference between cancer and non-cancer cell lines and the overall amount of chromatin-associated Y RNA molecules varied considerably between the different cell lines (Fig. 1B). However, the relative proportions of chromatin-associated Y RNAs varied little (Fig. 1C).

We conclude that chromatin-associated Y RNAs account for an average of 10–15% of the total Y RNA in a proliferating cell, independent of whether it is cancer-derived or not.

Y RNA levels are decreased in quiescence

Y RNAs are significantly overexpressed in human solid tumours compared to corresponding normal tissues (Christov et al., 2008), yet we found no significant difference in their amounts between proliferating human cancer and non-cancer derived cell lines. This raises the possibility that Y RNAs may in fact be downregulated in normal tissues, where most cells are quiescent and do not proliferate *in situ*, unlike tumour tissues or proliferating cell lines in culture. We therefore compared the absolute amounts of soluble and chromatin-associated Y RNA molecules in quiescent and proliferating cells (Fig. S1).

We induced quiescence in EJ30 bladder carcinoma, HCA-7 colon adenocarcinoma and hTERT-immortalised normal RPE-1 retinal pigment epithelial cells (Fig. S1A). There was an overall and significant 2–5-fold decrease in the total numbers of Y RNA molecules in the quiescent cells (P<0.03, unpaired two-tailed t-tests), which affected both soluble and chromatin-associated

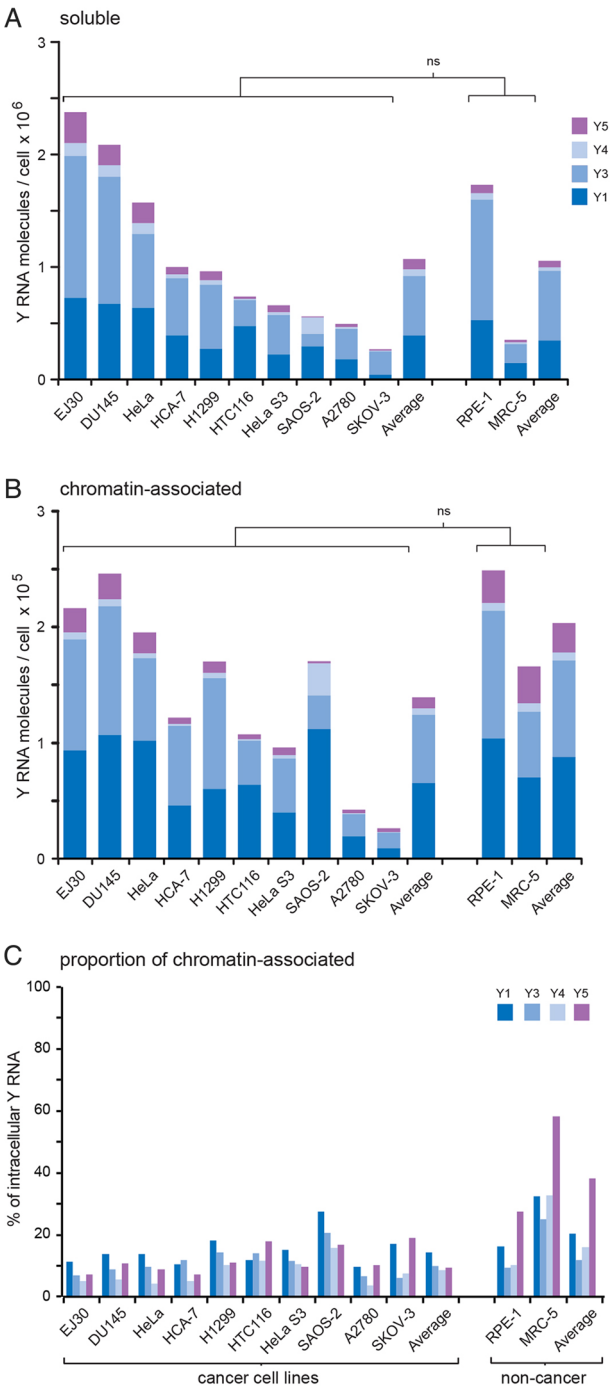

Fig. 1. Quantification of Y RNA levels in asynchronously proliferating human cell lines. The indicated cell lines were grown as asynchronously proliferating cultures. Total RNA was isolated from the (A) cytosolic and the (B) chromatin-associated fractions of these cell cultures. The absolute numbers of the indicated Y RNA molecules present in these intracellular fractions were determined by qPCR. Average values are shown for both cancer and non-cancer derived cell lines. Mean values of three independent experiments (n=3) are shown. Brackets indicate data grouped for statistical tests (i.e. cancer versus non-cancer); ns, not significant, P>0.3 (two-tailed t-tests). (C) Proportions of chromatin-associated Y RNAs. Individual Y RNAs are colour-coded as indicated.

Journal of Cell Science (2017) 130, 1239-1250 doi:10.1242/jcs.197566

cellular compartments equally (Fig. S1B–D). We conclude that Y RNA expression is systematically elevated in proliferating cells compared to quiescent ones. This upregulation is consistent with the essential function of Y RNAs during the initiation of chromosomal DNA replication (Christov et al., 2006; Krude et al., 2009).

Elevated levels of chromatin-associated Y RNAs during S phase

We next characterised the expression levels and intracellular partition of Y RNAs during the cell cycle. HeLa cells were synchronised at mitosis, in early-, mid- and late-G1, in early-, early/mid-, mid S- and late S/G2-phase. We confirmed cell synchrony by flow cytometry (Fig. 2A) and by determining the percentages of actively replicating cell nuclei (Fig. 2B).

The overall number of soluble Y RNA molecules per cell varied non-significantly between different the cell cycle phases (Fig. 2C). Y3 RNA was the most abundant in the soluble fraction, and the relative proportions of the four Y RNAs did not change during the cell cycle (Fig. 2C).

In contrast, the amounts of chromatin-associated Y RNAs per cell changed systematically and significantly during the cell cycle (Fig. 2D). The total numbers of chromatin-associated Y RNAs ranged between 300,000 and 500,000 molecules per cell in mitosis and G1 phase (Fig. 2D). As cells entered S phase, the number increased significantly to 950,000 in early S phase and reached 1.2 million molecules per cell in mid/late-S phase (Fig. 2D). Furthermore, the relative proportions of the four Y RNAs also changed as cells entered S phase. Y1 RNA became the most abundant (Fig. 2D) and the proportions of chromatin-associated Y1 and Y5 RNA increased substantially (Fig. 2E).

To substantiate these findings independently, we also quantified amounts of Y RNAs in soluble and chromatin-associated fractions in human EJ30 cells that were forced into quiescence by serum starvation and subsequently released into the proliferative cell cycle (Fig. S2A). As cells exited quiescence and traversed G1 phase for 13 h, the number of soluble and chromatin-associated Y RNAs increased ∼5-fold, suggesting that their expression is upregulated upon exit from quiescence into G1 phase (Fig. S2B). When cells had entered S phase by 25 h, the absolute numbers of soluble Y RNAs dropped while chromatin-associated Y RNAs increased 4-fold, leading to substantially increased proportions of chromatin-associated individual Y RNAs (Fig. S2B).

Taken together, our data suggest that the association of Y RNAs with the insoluble nuclear chromatin fraction is regulated during the cell cycle, resulting in a significantly increased proportion of Y RNAs associated with chromatin during S phase.

Increased association of Y RNAs with S phase chromatin *in vitro*

Previous *in vitro* studies revealed a rapid dynamic association of fluorescently labelled Y RNAs with chromatin in nuclei crossing the G1 to S phase boundary (Zhang et al., 2011). We adapted this

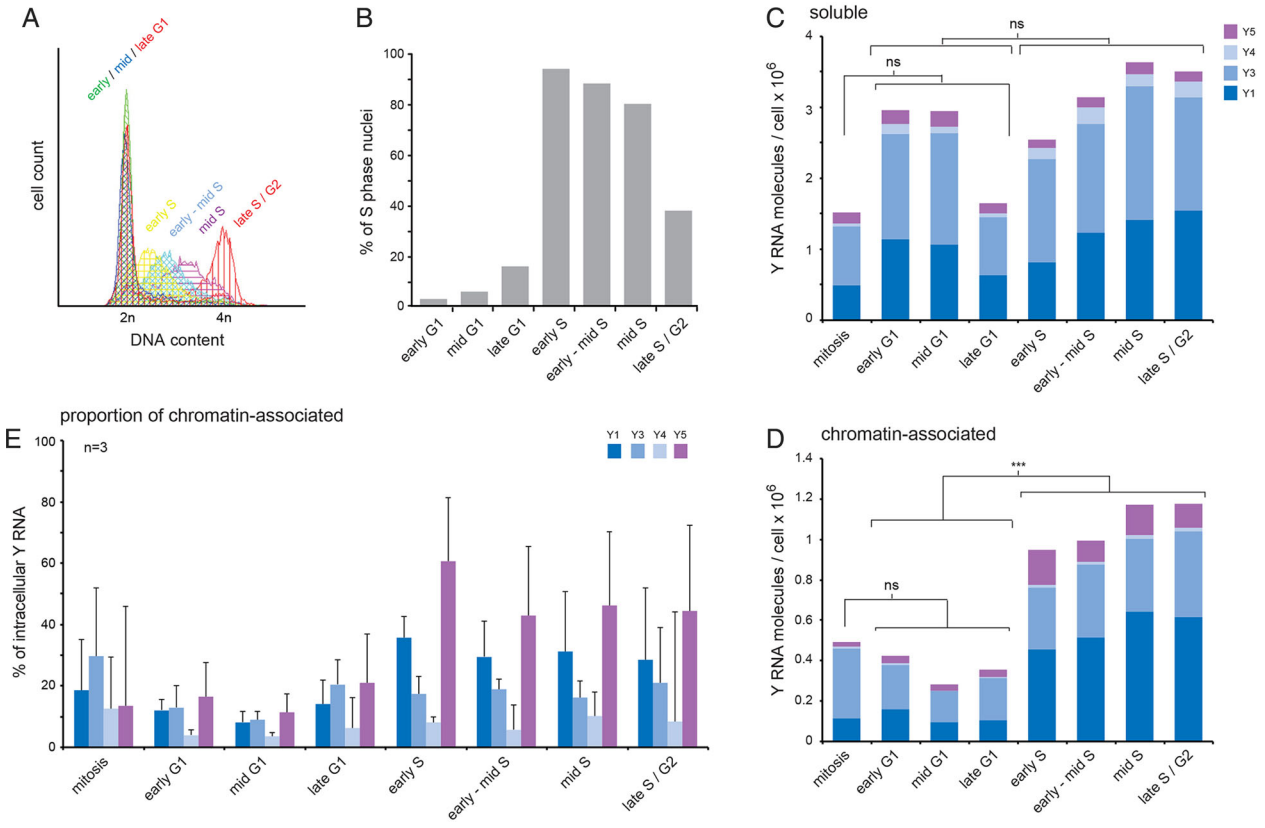

Fig. 2. Quantification of Y RNA levels during the cell cycle. HeLa cells were synchronised in the indicated phases of the cell cycle (see Materials and Methods). (A) Confirmation of cell synchrony by flow cytometry. A colour-coded overlay of individual flow cytometry profiles is shown; positions of unreplicated (2n) and fully replicated (4n) DNA content are indicated. (B) S phase indexes. Percentages of S phase nuclei were determined for each synchronised cell population by nuclear run-on replication *in vitro*. (C,D) Quantification of intracellular Y RNA levels. Total RNA was isolated from the (C) cytosolic and the (D) chromatin-associated fractions of the synchronised cells. Absolute numbers of the indicated Y RNA molecules were determined by qPCR. Brackets indicate data grouped for statistical tests (i.e. mitosis versus G1, G1 versus S). ***P<0.001; ns, not significant, P>0.05 (two-tailed t-tests). (E) Proportions of chromatin-associated Y RNAs. Mean±s.d. for three independent experiments (n=3) are shown.

Journal of Cell Science (2017) 130, 1239-1250 doi:10.1242/jcs.197566

assay to visualise and quantify the association of fluorescent Y RNAs to nuclei from synchronised HeLa cells (Fig. 3). We compared the chromatin binding of fluorescent Alexa-Fluor-488-labelled Y1 RNA with that of 5S rRNA and spliceosomal U2 snRNA. A substantial amount of Y1 RNA associated with G1 and S phase nuclei, whereas an association of U2 and 5S RNAs was barely detectable under these conditions (Fig. 3A). Next, we quantified this association by measuring the integrated fluorescence pixel density over the nuclear area (Fig. 3B). The mean binding of Alexa-Fluor-488-conjugated Y1 RNA to G1 and S phase nuclei was ∼20-fold higher than that of U2 or 5S rRNA, and the association of Y1 RNA was more efficient in S phase nuclei compared to G1 phase nuclei (Fig. 3B). We therefore quantified the association of Alexa-Fluor-488-labelled Y1 RNA with nuclei from synchronised cells at higher temporal resolution (Fig. 3C). The association of Y1 RNA with early-, mid- and late-S phase nuclei was significantly and 2-fold higher than with early to late-G1 phase nuclei, as indicated by the 2-fold increases of the means and medians between these distributions. We observed a similar effect with Alexa-Fluor-488-labelled Y5 RNA (data not shown). To independently confirm this analysis, we also measured the amounts of Y1 RNA associating *in vitro* with nuclei from EJ30 cells synchronised by serum starvation and release (Fig. S2C). Significantly increased amounts of Y1 associated with S phase nuclei *in vitro*, compared to quiescent or G1 phase nuclei.

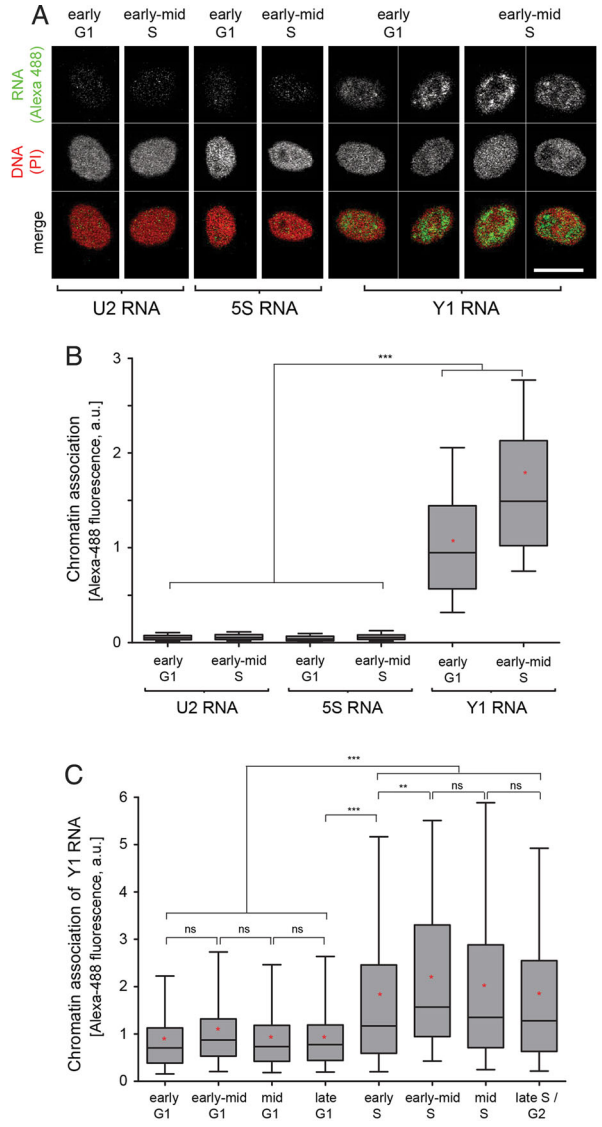

Fig. 3. Y1 RNA preferentially associates with S phase nuclei *in vitro*. Nuclei were prepared from synchronised HeLa cells and incubated *in vitro* with fluorescent Alexa-Fluor-488-labelled Y1 RNA, U2 RNA or 5S RNA and HeLa cytosolic extract for 1 min. Nuclei were fixed and the fluorescent Y RNAs associated with the nuclear structure were visualised by confocal fluorescence microscopy. (A) Representative micrographs showing association of U2, 5S and Y1 RNAs with G1 and S phase nuclei. Fluorescent Alexa-Fluor-488-labelled RNAs are shown in green and nuclear DNA is counterstained with propidium iodide (red). Scale bar: 10 µm. (B) Quantification of RNA binding to isolated cell nuclei. Alexa-Fluor-488-conjugated RNA fluorescence of the indicated RNAs was recorded by confocal microscopy, and integrated pixel density analysis was performed with ImageJ. Results of a representative binding experiment are shown as box-and-whisker plots. The box represents the 25–75th percentiles, and the median is indicated. The whiskers show the 5–95th percentiles; red asterisks indicate mean values. $n \geq 329$ nuclei for each sample. (C) Quantification of Y1 RNA binding to nuclei of synchronised cells. Y1 RNA association with the indicated nuclei was analysed as in B, $n \geq 457$ nuclei for each sample. Analysis of variance (one-way ANOVA) was used to determine significance of variance between groups; brackets indicate individual and grouped data sets used for ANOVA. $^{**}P \leq 0.01$; $^{***}P < 0.001$; ns, not significant, $P > 0.05$.

However, these quantitative RNA binding analyses are subject to caveats of cell synchronisation effects and technical variability between individual reactions. To circumvent these, we compared the binding of Alexa-Fluor-488-labelled Y1 RNA to nuclei of asynchronously proliferating HeLa cells within one reaction (Fig. S3A). S phase nuclei were identified by nuclear run-on replication taking place during the RNA-binding reaction *in vitro* and subsequent visualisation of DNA replication foci by immunofluorescence microscopy (Zhang et al., 2011). We observed a statistically significant 2-fold increase in the amount of Y1 RNA associating with S phase nuclei compared to non-S phase nuclei (Fig. S3B). Flow cytometry profiles indicated that non-S phase nuclei consist >95% of G1 phase and <5% of G2 phase (not shown).

Taken together, we conclude that significantly more Y RNA molecules associate with S phase nuclei than with G1 phase nuclei.

Y RNAs associate with early-replicating euchromatin in G1 phase

Y RNAs associate with unreplicated chromatin at the G1 to S phase transition (Zhang et al., 2011). We therefore investigated whether Y RNAs associate with particular DNA replication timing domains in G1 phase nuclei *in vitro* (Fig. 4).

To label replication timing domains, we pulse-labelled replicating DNA in asynchronously proliferating HeLa cells for 5 mins with 5-ethynyl-2-deoxuridine (EdU) *in vivo* and chased the cells without EdU for 11 h into the subsequent G1 phase. We isolated the nuclei and incubated them in the cell-free system with fluorescent Alexa-Fluor-488-labelled Y RNAs. S phase nuclei present in this reaction were identified by incorporation of digoxigenin-dUTP *in vitro*, and subsequently excluded from the analysis. Based on the patterns of replication foci pre-labelled in the previous S phase *in vivo* (Berezney et al., 2000), we were able to class replication timing domains in these G1 phase nuclei as early-, mid- or late-replicating. We then visualised and quantified the overlap between sites of associated Y RNAs and pre-labelled replication timing domains (Fig. 4).

Y1 and Y5 RNAs associated predominantly with early-replicating domains, and to a lesser extent, if at all, with mid- and late-replicating domains in G1 phase nuclei (Fig. 4A). We

Journal of Cell Science (2017) 130, 1239-1250 doi:10.1242/jcs.197566

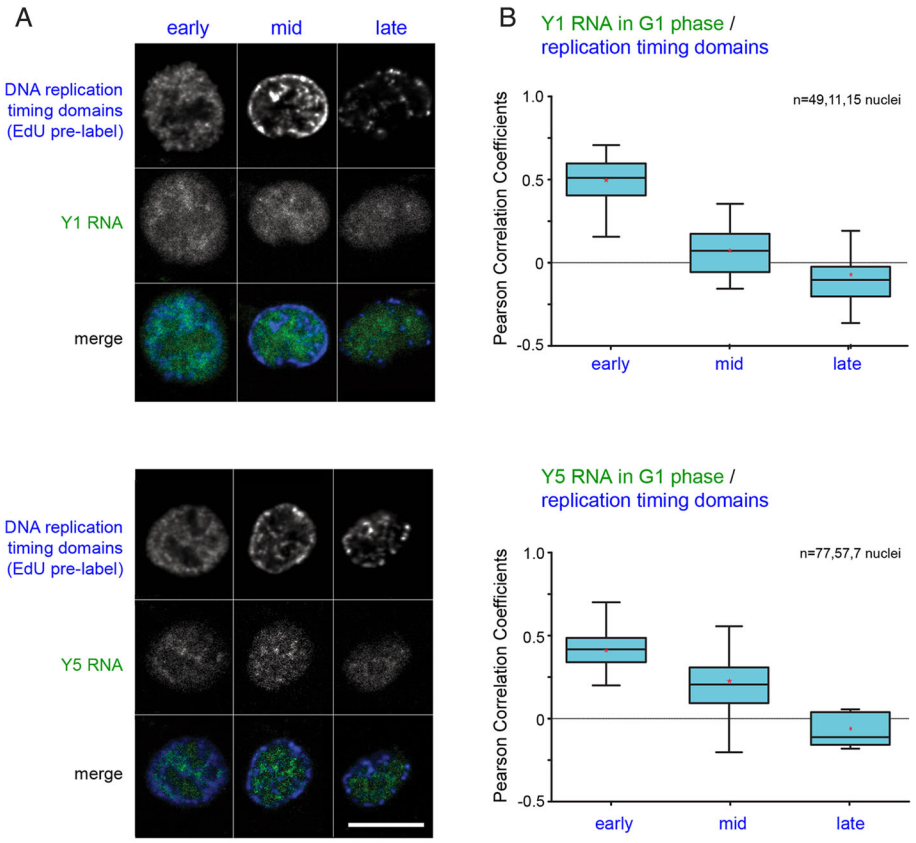

Fig. 4. Y RNAs associate with early-replicating euchromatin during G1 phase. (A) Chromatin association of Y RNAs with discrete DNA replication timing domains. To label replication timing domains, asynchronously proliferating HeLa cells were pulse-labelled *in vivo* with EdU for 5 min and chased into the subsequent G1 phase by adding EdU-free medium for 11 h. Nuclei were isolated and incubated with fluorescent Alexa-Fluor-488-labelled Y RNAs (green) and digoxigenin-dUTP in a cell-free DNA replication system for 5 min *in vitro*. EdU was detected using Click-it chemistry (blue) and digoxigenin-dUTP was detected using Rhodamine-conjugated anti-digoxigenin antibodies. G1 nuclei were identified by their absence of digoxigenin incorporation. Early-, mid- and late-replicating chromatin domains were identified by patterns of EdU pulse-labelled DNA replication foci (Berezney et al., 2000). Sites of chromatin-associated Y1 RNA (top panel) and Y5 RNA (bottom panel) were detected by using confocal fluorescence microscopy in G1 phase nuclei in comparison to replication-timing domains in these G1 phase nuclei (merge). Scale bar: 10 µm. (B) Quantitative colocalisation analysis. Pearson's correlation coefficients were determined for the pixel-by-pixel overlap between sites of chromatin-associated Y1 (top panel) or Y5 (bottom panel) RNA and early-, mid- and late-replicating chromatin domains in the G1 phase nuclei. Box-and-whisker plots of the Pearson's correlation coefficients are shown as in Fig. 3. Numbers of independent nuclei analysed for each dataset are indicated (*n*).

quantified the extent of colocalisation between sites of associated Y RNAs and the pre-labelled replication timing domains as Pearson correlation coefficients (Fig. 4B). Coefficients of 0.0 to ±0.19 are taken as no correlation, ±0.2 to ±0.29 as weak, ±0.3 to ±0.39 as moderate, ±0.4 to ±0.69 as strong, ±0.7 to ±0.99 as very strong and ±1 a perfect positive or negative correlation, respectively. Y1 and Y5 RNAs showed a strong positive correlation with early-replicating domains in G1 phase nuclei, but no or weak positive correlation with mid-replicating domains, and no or weak negative correlation with late-replicating domains (Fig. 4B).

We conclude that Y RNAs associate preferentially with early-replicating chromosome domains in G1 phase, whilst they are not enriched at mid- and late-replicating domains. Next, we investigated the dynamic association of Y RNAs with chromatin during S phase.

Y RNAs re-associate with replicated chromatin before the end of S phase

S phase is characterised by an elevated association of Y RNAs with chromatin (see Figs 2 and 3, Figs S2 and S3), yet chromatin-associated Y RNAs were seen to be excluded from sites of active DNA replication *in vitro* (Zhang et al., 2011). We therefore investigated whether Y RNAs are able to re-associate with replicated chromatin during later stages of S phase (Fig. 5). First, we pulse-labelled active sites of ongoing DNA replication in asynchronously proliferating HeLa cells with EdU, and chased the cells without EdU for 0, 2.5 and 5 h *in vivo*. Nuclei were then isolated and incubated *in vitro* for a second pulse-label with digoxigenin-dUTP in the presence of fluorescent Alexa-Fluor-488-labelled Y RNAs. Only S phase nuclei showing both replication labels were included in the analysis. The zero-time chase provides the positive control for a colocalisation of DNA replication foci active *in vivo* with those active after the isolation *in vitro*. Longer chase times will show selective marking of replicated chromatin domains with EdU in comparison to the active replication sites marked with digoxigenin-dUTP. We then investigated whether Y RNAs are present at sites of active DNA replication and associate with regions that were recently replicated during the same S phase.

In the zero hour control chase (Fig. 5A, left), intranuclear sites of DNA replication *in vivo* (blue) and *in vitro* (red) overlap and show a magenta colour in the merged images. Associated Y1 and Y5 RNA are excluded from these DNA replication sites and show a green pattern (Fig. 5A). After a 2.5 h chase (Fig. 5A, middle), sites of DNA replication *in vivo* and *in vitro* have diverged and display

Journal of Cell Science (2017) 130, 1239-1250 doi:10.1242/jcs.197566

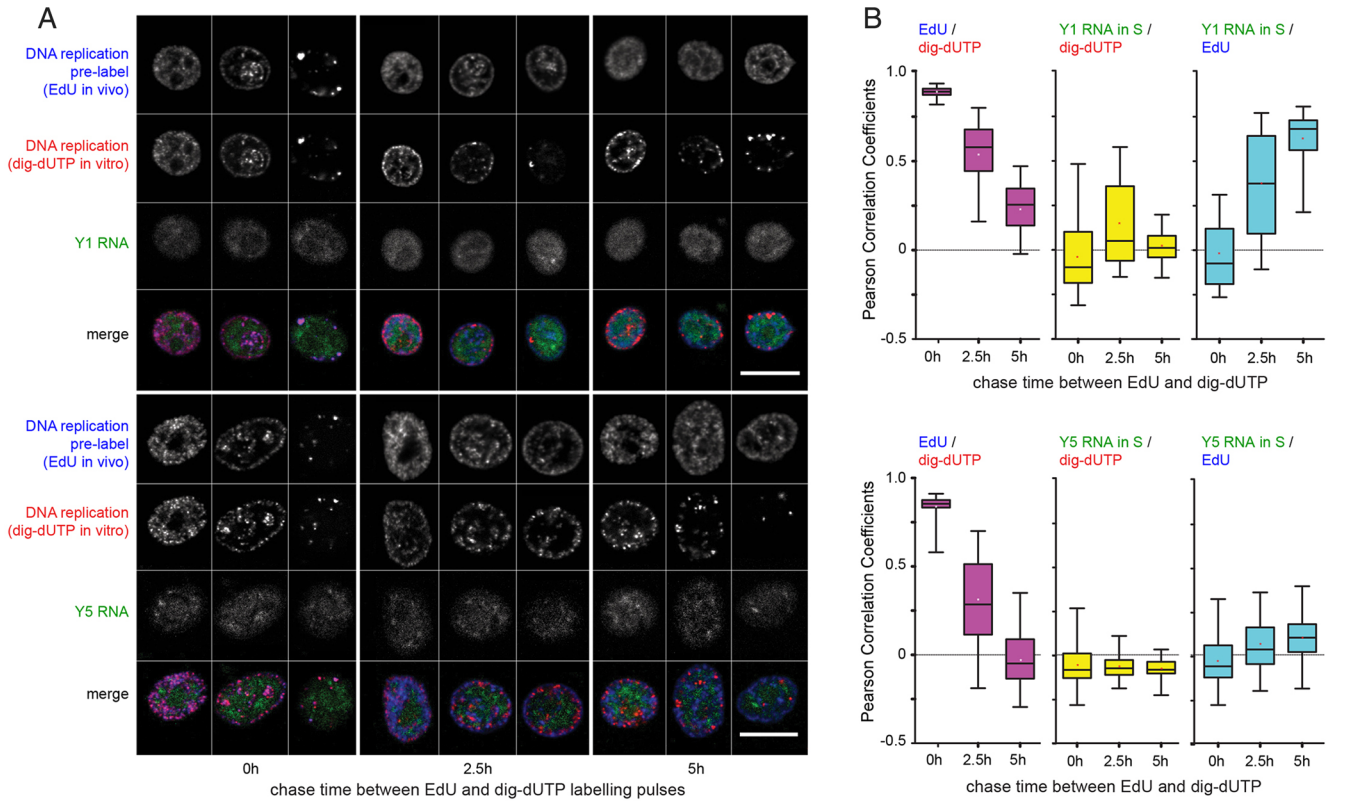

Fig. 5. Chromatin-binding dynamics of Y1 and Y5 RNA during S phase. To differentially label unreplicated, replicating and replicated chromatin domains, asynchronously proliferating HeLa cells were first pulse-labelled with EdU for 5 min *in vivo* and then chased by adding EdU-free medium for 0, 2.5 and 5 h. Nuclei were isolated and incubated in a cytosolic extract from proliferating HeLa cells supplemented with fluorescent Alexa-Fluor-488-labelled Y RNAs and digoxigenin-dUTP for 5 mins *in vitro*. (A) Confocal microscopy. Intranuclear sites of EdU (blue) and digoxigenin-dUTP incorporation (red) and associated Y1 and Y5 RNA (green) are shown for 0 h (left), 2.5 h (middle) and 5 h chase time (right). Scale bars: 10 µm. (B) Quantitative colocalisation analysis. Pearson's correlation coefficients were determined pairwise for the pixel-by-pixel overlap between sites of EdU and digoxigenin pulses (left column), and between chromatin-associated Alexa-Fluor-488-labelled Y1 (top row) or Y5 (bottom row) RNA, and sites of digoxigenin-dUTP (middle column) and EdU pulses (right column). Box-and-whisker plots of the Pearson's correlation coefficients are shown. The box represents the 25–75th percentiles, and the median is indicated. The whiskers show the 5–95th percentiles; asterisks indicate mean values. 100 nuclei were analysed for each time point.

separate foci for already replicated and actively replicating DNA, respectively. Y RNAs were found to be mostly associated with non-replicating sites (green), but some overlap with replicated sites became also apparent (cyan). After a 5 h chase (Fig. 5A, right), the DNA replication sites labelled *in vivo* and *in vitro* have completely diverged, revealing blue and red foci, respectively. Y RNAs appeared mostly on non-replicating chromatin (green) but were also found at sites that had already replicated *in vivo* (cyan), in particular in those nuclei that were in early S phase during the first pulse. Taken together, these observations suggest that Y RNAs are able to associate with replicated chromatin in these nuclei.

To substantiate these observations, we quantified the overlap between these sites by determining the pairwise Pearson correlation coefficients of the three labels (Fig. 5B). Sites of replicated chromatin *in vivo* and *in vitro* were very strongly positively correlated for the zero hour chase and declined to moderate and eventually very low or no correlation with increasing chase time (Fig. 5B, left panels). Importantly, no correlation was detected between associated Y1 or Y5 RNAs with sites of ongoing DNA replication (Fig. 5B, middle panels and 0 h chase, right panels), consistent with earlier observations (Zhang et al., 2011). Strikingly, sites of associated Y1 RNA correlated moderately and strongly with sites of replicated chromatin at the 2.5 and 5 h chase time, respectively (Fig. 5B, top right panel). The correlation of sites of Y5 RNA association with replicated chromatin increased only slightly, but discernibly, during this time (Fig. 5B, bottom right panel).

We conclude that Y RNAs re-associate with replicated chromatin during S phase within a few hours after it has been replicated, and Y1 RNA re-associates more efficiently with these replicated domains than Y5 RNA.

Chromatin association dynamics of Y RNAs are in concordance with those of ORC

Y RNAs interact biochemically with DNA replication initiation proteins, including ORC and the pre-RC proteins Cdt1 and Cdc6, and they colocalise with these proteins and MCM2-7 on unreplicated chromatin at the G1 to S phase transition (Collart et al., 2011; Zhang et al., 2011). We therefore investigated whether the dynamic association of Y RNAs with chromatin during S phase is mirrored by the association dynamics of ORC, the pre-RC or other replication fork-associated proteins. We used the same pulse-labelling approach as in Fig. 5, but detected sites of candidate proteins by indirect immunofluorescence microscopy (Fig. 6; Fig. S4A).

Sites of chromatin-associated ORC (subunits ORC2 and ORC3) did not correlate with sites of ongoing DNA replication (Fig. 6A,B; Fig. S4A). Like Y RNAs, ORC re-associated with replicated chromatin domains a few hours after their replication during the same S phase (Fig. 6A,B; Fig. S4A). The pre-RC proteins Cdc6 and

Journal of Cell Science (2017) 130, 1239-1250 doi:10.1242/jcs.197566

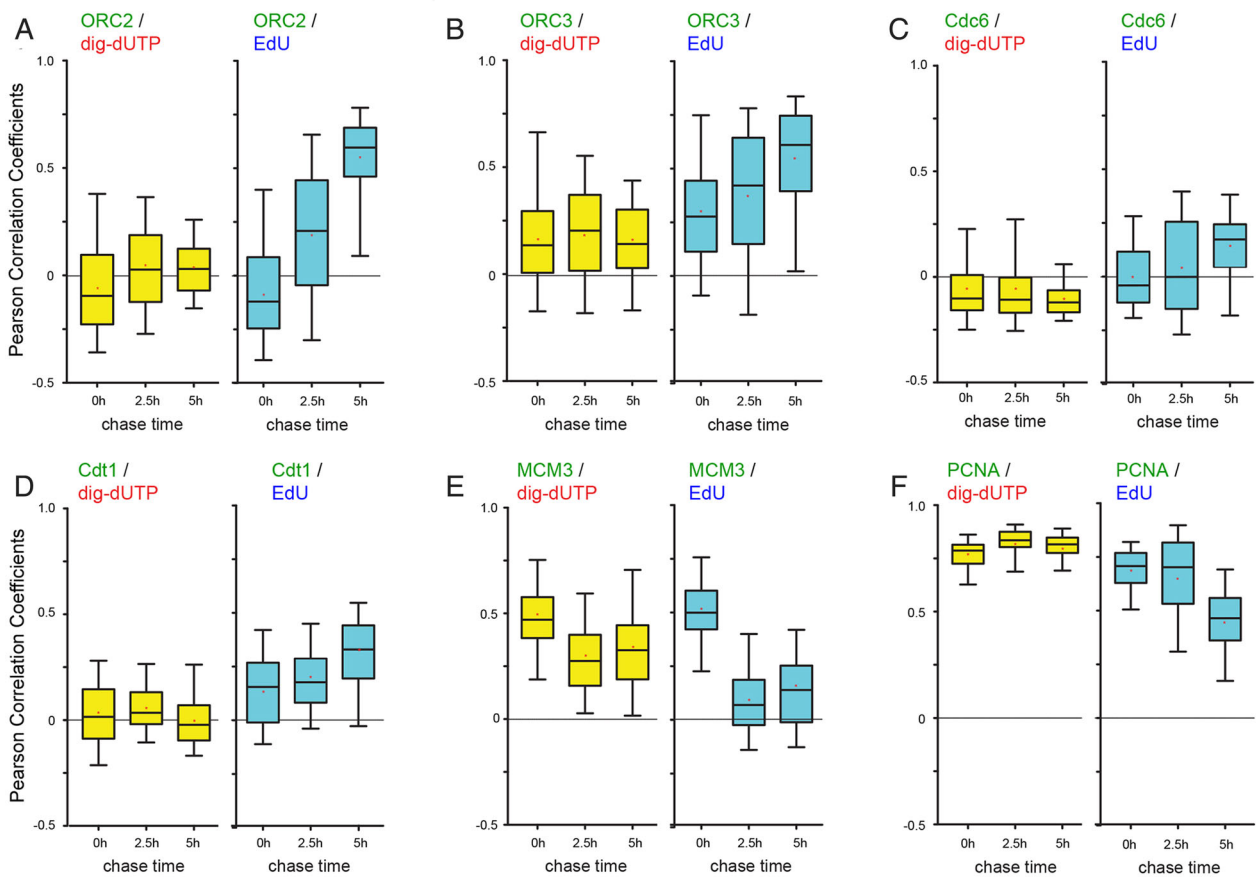

Fig. 6. Chromatin-binding dynamics of replication proteins during S phase. The intranuclear sites of chromatin-associated replication proteins were determined by indirect immunofluorescence microscopy in relation to sites of replicated (EdU) and replicating chromatin (digoxigenin-dUTP), as detailed for Y RNAs in Fig. 5. Quantitative colocalisation analysis of Pearson's correlation coefficients was performed pairwise for the pixel-by-pixel overlap between sites of (A) ORC2, (B) ORC3, (C) Cdc6, (D) Cdt1, (E) MCM3 and (F) PCNA with sites of digoxigenin-dUTP (left columns) and EdU pulses (right columns). Box-and-whisker plots of the Pearson's correlation coefficients are shown as in Fig. 5; 100 nuclei were analysed for each time point. Representative confocal immunofluorescence micrographs of the association analysis of ORC2 and ORC3 are shown in Fig. S4A.

Cdt1 also did not localise to sites of ongoing DNA replication, but then did not re-associate effectively with replicated chromatin (Fig. 6C,D). The pre-RC and replicative DNA helicase subunit MCM3 correlated moderately with active replication foci but did not do so with replicated chromatin domains (Fig. 6E), consistent with its role as a licensing factor. Finally, sites of the replication fork protein PCNA correlated very strongly with active DNA replication foci and the correlation decreased to moderately low levels with replicated domains (Fig. 6F).

In conclusion, the chromatin association dynamics of the non-coding Y RNAs are in concordance with those of ORC, but not with those of the pre-RC or replication-fork-associated proteins.

Y1 RNA colocalises with the chromatin-associated ORC during the cell cycle

In the final experiments, we investigated the colocalisation of replication proteins with Y1 and Y5 RNAs in isolated cell nuclei throughout the cell cycle.

We observed a strong positive correlation of the chromatin association sites of ORC2 and ORC3 with Y1 RNA at all points of the cell cycle, but not with Y5 RNA (Fig. 7A,B; Fig. S4B). This corroborates the idea that there is a functional interaction between Y1 RNA and ORC, as suggested by previous biochemical interaction and chromatin-binding studies (Collart et al., 2011; Zhang et al., 2011). In contrast, sites of Cdc6 protein did not correlate with the location of Y1 or Y5 RNAs at any stage of the cell cycle (Fig. 7C). Similarly, sites of Cdt1 protein did not correlate with the location of Y1 RNA, but generally showed a weak positive correlation with Y5 RNA (Fig. 7D). The sites of MCM3 protein correlated moderately positively with Y1 RNA in non-S and early-S phase nuclei but did not do so in mid- and late S-phase (Fig. 7E), when MCM proteins become displaced locally from replicated chromatin under these conditions (Krude et al., 1996). We observed no correlation of MCM3 protein sites with Y5 RNA during the entire cell cycle.

Furthermore, sites of the replication fork protein PCNA and of the heterochromatin protein HP1α (also known as CBX5) did not correlate with Y1 or Y5 RNAs at any time of the cell cycle (Fig. 7F,G), demonstrating that Y RNAs do not associate preferentially with replication forks or heterochromatin domains at any time.

Interestingly, the association of Y RNAs with nucleoli regions differed between the two Y RNAs (Fig. 7H). Sites of Y1 RNA appeared to be excluded from sites of nucleolin protein (Fig. S4C) and these sites showed no, or very weak negative correlation throughout the cell cycle (Fig. 7H). In contrast, sites of Y5 RNA overlapped visually with nucleolin in non-S and early-S phase (Fig. S4C), and these sites correlated positively and strongly at these stages (Fig. 7H). This positive correlation decreased at the time when these nucleolar sites replicated in mid-S phase (Fig. S4C), and eventually reached no correlation in late-S phase (Fig. 7H).

Journal of Cell Science (2017) 130, 1239-1250 doi:10.1242/jcs.197566

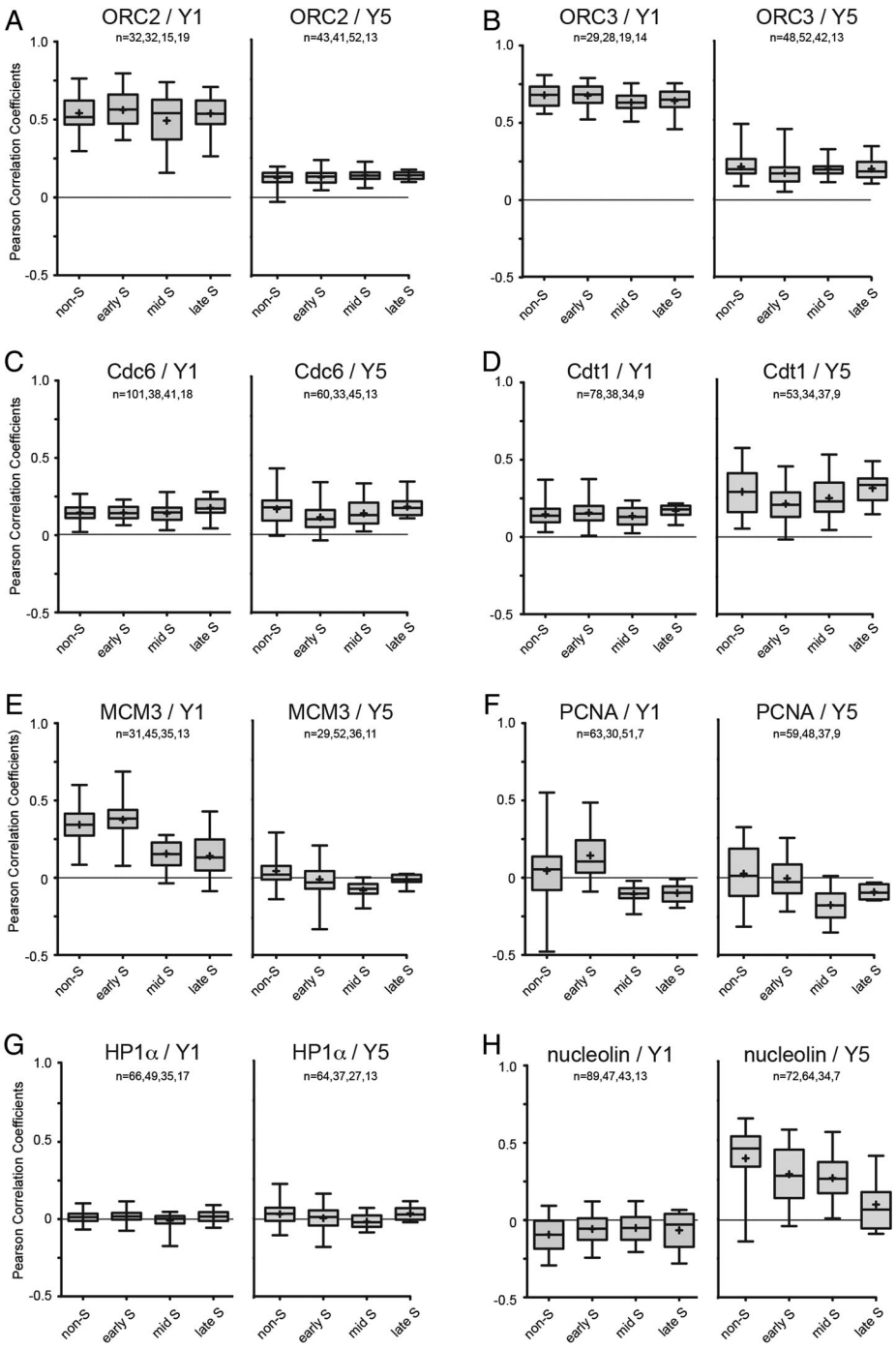

Fig. 7. Colocalisation of replication and chromatin marker proteins with Y1 and Y5 RNAs during the cell cycle. Asynchronously proliferating HeLa cells were pulse-labelled with EdU for 5 min before isolating their nuclei. Nuclei were incubated in cytosolic extract from proliferating HeLa cells supplemented with fluorescent Alexa-Fluor-488-labelled Y1 or Y5 RNA for 1 min. EdU was detected using Click-it chemistry and nuclei were sorted by their replication patterns into early-, mid- and late-S phase; a lack of EdU incorporation was taken as non-S phase. Quantitative colocalisation analysis of Pearson's correlation coefficients was performed pairwise for the pixel-by-pixel overlap between sites of (A) ORC2, (B) ORC3, (C) Cdc6, (D) Cdt1, (E) MCM3, (F) PCNA, (G) heterochromatin protein HP1α and (H) nucleolin with sites of Y1 RNA (left columns) and Y5 RNA (right columns). Box-and-whisker plots of the Pearson's correlation coefficients are shown as in Fig. 5; the numbers of nuclei analysed for each time point are indicated (*n*). Representative confocal immunofluorescence micrographs of the colocalisation analysis of Y RNAs with ORC3 and nucleolin are shown in Fig. S4B,C.

In conclusion, Y1 RNA shows highly concordant chromatin association dynamics to that of ORC throughout the cell cycle. Y5 RNA associates preferentially with sites of unreplicated nucleoli, suggesting that these two Y RNAs may be involved in different nuclear processes.

DISCUSSION

In this paper, we provide a quantitative analysis of Y RNA levels in a panel of human cells and of their intracellular partition into soluble and chromatin-associated cellular fractions. We have used two independent approaches: (1) qPCR and (2) chromatin-association of fluorescently labelled Y RNAs in a physiological cell-free system. We found that overall Y RNA levels are comparable between proliferating cancer and non-cancer cells, but decrease substantially in quiescent cells. Compared to G1 phase, 2- to 4-fold increased amounts of Y RNAs associate with euchromatin during S phase, both with unreplicated chromatin in early S and again with replicated chromatin in late S. The chromatin association dynamics of Y1 RNA mirrors those of ORC.

Y RNA abundance

Since their discovery in the early 1980s (Hendrick et al., 1981; Lerner et al., 1981), Y RNAs have been described as relatively abundant small RNAs. Here, we have used cell fractionation and qPCR to determine the absolute numbers of Y RNA molecules in a panel of human cells. We found that overall Y RNA amounts varied

Journal of Cell Science (2017) 130, 1239-1250 doi:10.1242/jcs.197566

non-systematically between human cell lines with an overall number of ∼1.3 million Y RNA molecules per cell, ranging between 0.3 and 2.5 million for different cell lines. Compared to other species, this number is in range of the ∼1 million Y RNA molecules per *Xenopus laevis* egg and exceeds the ∼0.1 million per zebrafish egg (Collart et al., 2011). These numbers remain constant per embryo after fertilisation until the mid-blastula transition (MBT) in both species, so that the actual number of molecules per cell decreases during these early embryonic cycles. After the MBT, when Y RNA become essential for DNA replication, cell proliferation and embryo viability (Collart et al., 2011), the amounts of Y RNAs per embryo increase through induction of zygotic transcription of the Y RNA genes to compensate for the increasing number of cells per embryo (Collart et al., 2011). Any quantitative differences between these three different datasets will be influenced by differences between species and by different protocols of RNA extraction and qPCR quantification. The relatively high expression levels of Y RNA in vertebrate cells suggest that they may exert their physiological function in a structural or stoichiometric manner, or that they are present in excess of their physiological requirements.

Y RNA expression and cancer

An earlier investigation of relative Y RNA abundance in human cancer tissues by qPCR established that Y RNAs were more abundant in human solid tumours than in corresponding normal tissues (Christov et al., 2008). Our data reported here offer a physiological explanation for this observation. We found that overall expression levels of Y RNAs do not differ significantly between different proliferating cell lines of cancer and non-cancer origin. In contrast, Y RNA levels are significantly reduced in quiescent cells, and their expression is induced when quiescent cells enter the proliferative cell cycle. Therefore, elevated Y RNA levels in solid tumour samples can best be explained by the higher proportions of proliferating cells in tumours than in corresponding normal tissues. As consequence, we propose that elevated Y RNA levels should not necessarily be regarded as a cancer marker, but as a potential cell proliferation marker.

Chromatin association of Y RNAs

Early determinations of intracellular localisation and partitioning of Y RNAs between cytoplasm and nucleus have given varied results (reviewed by Hall et al., 2013; Kowalski and Krude, 2015; Pruijn et al., 1997). Northern blotting after enucleation and cell fractionation indicated that Y RNAs were predominantly, if not exclusively, cytoplasmic in *Xenopus laevis* oocytes and cultured mammalian cells (Gendron et al., 2001; O'Brien et al., 1993; Peek et al., 1993; Simons et al., 1994). However, *in situ* hybridisation and electron microscopy in cultured human cells showed discrete sites of Y RNAs in the nucleus and the cytoplasm (Farris et al., 1997; Matera et al., 1995). Physiological binding studies then demonstrated that Y RNAs associate efficiently with chromatin *in vitro* (Zhang et al., 2011). A conclusion from these studies is that Y RNA expression levels and their intracellular partition are found to vary depending on the methodologies used for their detection, and on the physiological state of the cells investigated (Kowalski and Krude, 2015).

In this paper, we provide the first comprehensive quantitative analysis of intracellular human Y RNAs during the cell cycle. We obtained mutually consistent results by cell fractionation and qPCR, and by association assays using fluorescently labelled Y RNAs. About 10% of total Y RNA was associated with chromatin in asynchronously proliferating cells, requiring an extraction with 0.5 M salt to isolate them from the nuclear structure. In synchronised cells, the amount of chromatin-associated Y RNA is 2- to 4-fold higher in S phase compared to in G1 phase or mitosis. We were not able, however, to investigate homogenous G2 phase cells as preparations were always contaminated with significant amounts of late S phase cells, due to the very short relative duration of G2 phase in the cells investigated. We would therefore propose that the preferential association of Y RNAs with S phase chromatin might suggest a functional involvement with replicating chromatin, consistent with the established essential role of Y RNAs for the initiation step of DNA replication (Christov et al., 2006, 2008; Collart et al., 2011; Gardiner et al., 2009; Kowalski and Krude, 2015; Krude et al., 2009; Wang et al., 2014).

In human cells, ∼30,000 replication origins become activated during S phase (Berezney et al., 2000; Huberman and Riggs, 1968), out of a pool of many more potential origins (Fragkos et al., 2015). We determined here that in synchronised human (HeLa) cells, about one million Y RNA molecules are associated with chromatin throughout S phase. Therefore, an order-of-magnitude excess of Y RNA molecules would be associated with chromatin per activated replication origin at any stage of S phase.

Our fluorescence-based Y RNA-binding studies showed a preferential association of Y RNAs with early-replicating euchromatin and not with late-replicating heterochromatin marked by HP1α protein *in vitro*. We also observed a positive overlap correlation with sites of associated ORC, supporting a reported biochemical interaction between ORC and Y RNAs (Zhang et al., 2011; Collart et al., 2011). It is currently unknown whether Y RNAs associate with early-firing replication origins in the human genome directly, or if they associate in a more disperse manner across early-replicating chromosome domains. A recent genome-wide mapping of ∼25,000 replication origins activated in a Y RNA-dependent manner *in vitro* located these origins as being predominantly in early-replicating chromosome domains (Langley et al., 2016). Therefore, sites of Y RNA association, and sites where their function is executed, appear to converge on early-replicating euchromatin. Systematic mutagenesis indicated that a specific association of Y1 RNA with open chromatin involves the loop domain (Zhang et al., 2011). Future technology development would be therefore required to enable genome-wide mapping of the sites of chromatin-associated Y RNA at higher resolution.

All four Y RNAs are functionally redundant with each other, with the presence of at least one type of Y RNA being essential for DNA replication initiation (Christov et al., 2006, 2008; Collart et al., 2011; Gardiner et al., 2009; Kowalski and Krude, 2015; Krude et al., 2009; Wang et al., 2014). They associate with open chromatin *in vitro* (Zhang et al., 2011) and, in competitive *in vitro* binding assays, human Y1, Y3 and Y4 RNA were shown to colocalise on open chromatin with each other after binding to chromatin. Y5 RNA also colocalised with Y1 RNA, but also showed association with additional sites overlapping nucleoli. Therefore, we investigated Y1 RNA (representing the collective behaviour of Y1, Y3 and Y4 RNAs) and Y5 RNAs separately here. In addition to an association with euchromatic sites, Y5 RNA also colocalised with nucleolin on nucleolar chromatin domains in G1 and S phase until the time of their replication in mid/late-S phase, when Y5 RNA was displaced from these sites locally. Nucleolin is a multifunctional protein with roles in rRNA processing, ribosome biogenesis and nucleo-cytoplasmic transport (Ginisty et al., 1999). It binds to the loop domain of Y RNAs and can form cytosolic ribonucleoproteins (RNPs) with all four Y RNAs in human cells (Fabini et al., 2001;

Journal of Cell Science (2017) 130, 1239-1250 doi:10.1242/jcs.197566

Langley et al., 2010). However, the interaction between Y RNAs and soluble nucleolin is not required for Y RNA function in DNA replication, as RNPs containing Y RNA and nucleolin can be immunodepleted from human cell extracts without compromising their ability to initiate DNA replication *in vitro* (Langley et al., 2010). Human Y5 RNA interacts with the ribosomal protein L5 (Hogg and Collins, 2007), which also associates with 5S rRNA (Steitz et al., 1988). Therefore, in addition to its conserved function in DNA replication, Y5 RNA may also have a second role in nucleolar function, possibly in rRNA biogenesis. Such a diversification of function would further support the modular nature of Y RNAs (Kowalski and Krude, 2015).

Are Y RNAs licensing factors?

In nuclei of cells synchronised at the G1 to S phase transition, Y RNAs were seen bound to chromatin prior to initiation of DNA replication, but became absent from active replication foci after replication was initiated *in vitro* (Zhang et al., 2011). Because Y RNAs are functionally essential for the initiation step (Christov et al., 2006; Krude et al., 2009), it was proposed that they may act in a manner consistent with the 'activator' function of the original 'licensing factor' model of 'once per cell cycle' control of origin firing (Zhang et al., 2011). In this model (Blow et al., 1987; Laskey et al., 1981), the 'activator' or 'licensing factor' binds to and marks unreplicated chromatin in G1 phase, and it is required for initiation of DNA replication. Following origin activation, it is then displaced from the origin site after initiation and prevented from rebinding to replicated DNA until the subsequent G1 phase, thus limiting initiation to once per cell cycle. Our data reported here clearly dismiss the hypothesis that Y RNAs are licensing factors as a substantial fraction of Y RNAs re-associates with replicated chromatin during later stages of S phase, which is inconsistent with the established activity of a licensing factor.

Concordant dynamics for Y RNAs and ORC

The hetero-hexameric ORC is conserved in eukaryotes and directs the assembly of the pre-replication complex at replication origins by a stepwise assembly with Cdc6, MCM2-7 and Cdt1 on chromosomal DNA (Costa et al., 2013; Fragkos et al., 2015; Siddiqui et al., 2013). The crystal structure of *Drosophila* ORC showed that five subunits (ORC1, 2, 3, 4 and 5) form a stable ring-shaped structure that can encircle DNA, whilst the ORC6 subunit is more loosely associated (Bleichert et al., 2015). Following pre-RC assembly in G1 phase, ORC disassembles partially as ORC1 is degraded while ORC2–6 remains stable and keeps an association with chromatin (Méndez et al., 2002; Tatsumi et al., 2003). The association of human ORC with chromatin and replication origins is regulated during the cell cycle, showing increased association in G1/S compared to G2/M phases (Gerhardt et al., 2006; Prasanth et al., 2004; Siddiqui and Stillman, 2007). ORC3 shows no obvious colocalisation with replication foci suggesting a displacement from replicating chromatin; however, in late S phase cells a weak and apparently euchromatic population of ORC3 remains detectable (see figure 6 of Siddiqui and Stillman, 2007). Here, we compared the chromatin association dynamics of human Y RNAs with ORC2 and ORC3 subunits during cell cycle progression and found that these were highly and significantly correlated between Y1 RNA and ORC2/3. Furthermore, Y RNAs do not colocalise with replication foci, as seen independently previously (Zhang et al., 2011), suggesting a temporal and local displacement during replication.

ORC interacts biochemically with immobilised Y RNAs in human nuclear extracts (Collart et al., 2011; Zhang et al., 2011), demonstrating stable direct or indirect physical interactions. Importantly, antisense morpholino oligonucleotides against Y RNAs inhibited Y RNA-dependent initiation of DNA replication and the biochemical interaction between Y RNAs and ORC (Collart et al., 2011). Therefore, ORC and Y RNAs are likely to interact in a common functional pathway, leading to the initiation of DNA replication. Several non-coding RNAs have been shown to facilitate recruitment of ORC to specific replication origin sites on chromosomal DNA in *Tetrahymena* and Epstein Barr virus (Mohammad et al., 2007; Norseen et al., 2008). In contrast, Y RNAs are actually recruited to chromatin themselves in an ORC-dependent manner in developing *Xenopus* embryos after the MBT (Collart et al., 2011). These observations suggest an ORC-dependent function for Y RNAs that is not related to the recruitment of ORC to replication origins. It is also unlikely that Y RNAs are required for the recruitment of the replicative helicase comprising MCM2-7 as part of the licensing reaction because this can be achieved with purified proteins in the absence of Y RNAs, at least in budding yeast (Yeeles et al., 2015). It is thus conceivable that Y RNAs are involved in another ORC-dependent aspect of chromatin dynamics during the initiation of DNA replication, and future work is therefore required to elucidate the molecular mechanisms of this pathway.

MATERIALS AND METHODS

Cell culture and synchronisation

All human cell lines were grown as monolayers in Gibco Dulbecco's modified Eagle's medium (DMEM; Invitrogen), supplemented with 10% fetal bovine serum (FBS; Invitrogen) and 1% penicillin-streptomycin (PAA) at 37°C and 10% CO_2 as detailed previously (Krude et al., 1997). Cells were free of microbial contamination. Detailed specifications are shown in Table S1.

HeLa cells were chemically synchronised at different points of the mitotic cell cycle by releasing from a double thymidine block (two times 24 h at 2.5 mM thymidine, separated by 12 h without thymidine) as detailed previously (Krude et al., 1997). G1 phase cells were acquired by releasing from double thymidine block for 12, 15 and 18 h to give early-, mid- and late-G1 cells, respectively. S and G2 phase cells were obtained by releasing them from a double thymidine block for 0.5, 2.5, 5.5 and 7 h to give early-S, early/mid-S, mid-S and late-S/G2 cells, respectively. Mitotic cells were obtained by an 11 h release from a double thymidine block into medium containing 40 ng/ml nocodazole (Calbiochem).

EJ30 and HCA-7 cells were forced into quiescence through serum starvation in DMEM containing 0.5% FBS for 15 days (Krude, 1999), while quiescence was achieved in RPE-1 cells by contact inhibition through cultivating confluent cells in DMEM containing 10% FCS for 7 days. Quiescent cells were released into the proliferative cell cycle by sub-cultivation at five times lower cell densities in fresh DMEM containing 10% FBS.

Synchronisation was confirmed by flow cytometry of isolated nuclei stained with propidium iodide, and S phase indices were determined by run-on replication of isolated nuclei incubated in a cytosolic extract from proliferating HeLa cells for 5 mins in the presence of digoxigenin-dUTP (Christov et al., 2006).

Cell fractionation and Y RNA quantification

Cells were fractionated into nuclei and cytosol by hypotonic treatment, dounce homogenisation and centrifugation at 3000 ***g*** as described previously (Zhang et al., 2011). To allow quantification of associated RNAs on a per cell basis, the total volumes of cell lysates were recorded and the concentrations of nuclei were determined on a haemocytometer after dounce homogenisation. Cell cycle positions were determined by flow cytometry of isolated nuclei. To prepare nuclear extracts, pelleted nuclei were resuspended in five times their volume of hypotonic buffer containing 0.5 M NaCl and incubated under continuous agitation for 30 min at 4°C. Nuclei were pelleted again at 16,000 ***g*** for 30 min and removed.

Total RNA was isolated from the cytosolic and the nuclear extracts by phenol extraction and ethanol precipitation, and their concentrations were

measured by nanodrop spectrophotometry as detailed previously (Zhang et al., 2011). Y RNAs in these extracts were quantified by qPCR using human Y RNA-specific primer pairs (Christov et al., 2006). Serial dilutions of known quantities of human Y RNA-encoding plasmid DNA molecules were used as specific calibrators for each Y RNA-specific qPCR. Absolute numbers of Y RNA molecules present per cell in the soluble cytosolic and nuclear extracts were calculated using the information on total yield volumes of lysates and fractionated extracts, and of nuclear concentrations in the lysates. For the calculations, we assumed 100% efficiency of cDNA synthesis. Proportions of chromatin-associated Y RNAs were determined as the amount of chromatin-associated Y RNAs over the sum of the amounts of soluble and chromatin-associated Y RNAs.

Synthesis of Y RNAs

Synthesis, purification and coupling of human Y1 and Y5 RNAs to Alexa Fluor 488 (Invitrogen) was performed exactly as described previously (Zhang et al., 2011).

Association of fluorescent Y RNAs with chromatin *in vitro* and colocalisation analyses

For pre-labelling of DNA replication sites *in vivo*, asynchronously proliferating HeLa cells were pulse-labelled with 10 µM 5-ethynyl-2-deoxuridine (EdU, Invitrogen) for 5 min *in vivo*, with or without further chase in the absence of EdU before the isolation of cell nuclei.

The chromatin association of fluorescent Y RNAs *in vitro* was quantified as described previously (Zhang et al., 2011). Briefly, isolated cell nuclei (0.6×10^6 –1×10^6 nuclei per reaction) were incubated for 1 min at 37°C with 300 ng of Alexa-Fluor-488-conjugated Y1 or Y5 RNA in physiological buffer with cytosolic extract of asynchronously proliferating HeLa cells (150 µg protein per reaction) and 150 pmol digoxigenin-dUTP (Roche). Nuclei were fixed with 4% paraformaldehyde and spun onto polylysine-coated glass coverslips. EdU was detected by using the Click-it imaging kit (Invitrogen) and dig-dUTP was detected using Rhodamine-conjugated anti-digoxigenin antibodies (Boehringer Mannheim), as described previously (Zhang et al., 2011). Nuclear proteins were detected by indirect immunofluorescence microscopy in the presence of RNase inhibitor (Zhang et al., 2011). Primary antibodies against the following proteins were used: ORC2, ORC3, MCM3 (all from Aloys Schepers, Helmholtz Centre Munich, Germany, 1:500 dilution); nucleolin (from Hans Stahl, University of Homburg, Germany, 1:500 dilution); Cdt1 (H-300, sc28262, Santa Cruz Biotechnology, 1:200 dilution); Cdc6 (H-304, sc8341, Santa Cruz Biotechnology, 1:500 dilution); PCNA (PC10, sc-56, Santa Cruz Biotechnology, 1:50 dilution); HP1α (clone 15.19s2, 05-689, EMD Millipore, 1:200 dilution). Chromosomal DNA was counterstained with propidium iodide or DAPI. Confocal fluorescence microscopy was performed on a Leica SP1 microscope using 63× objective lens magnification with a pinhole setting of 90 µm. Colocalisation was quantified by determining thresholded Pearson correlation coefficients using Volocity 6.3 software from Perkin Elmer.

Acknowledgements

We thank David Szüts and Christo Christov for critical reading of the manuscript. The University of Cambridge Department of Zoology confocal microscopy suite was financed by the Wellcome Trust and the Isaac Newton Trust.

Competing interests

The authors declare no competing or financial interests.

Author contributions

E.K. designed the study, performed the experiments and analysed the data; T.K. designed the study, analysed the data and wrote the manuscript.

Funding

This work was supported by the Association for International Cancer Research (AICR) (project grant 10-0570).

Supplementary information

Supplementary information available online at http://jcs.biologists.org/lookup/doi/10.1242/jcs.197566.supplemental

References

Arias, E. E. and Walter, J. C. (2007). Strength in numbers: preventing rereplication via multiple mechanisms in eukaryotic cells. *Genes Dev.* **21**, 497-518.

Berezney, R., Dubey, D. D. and Huberman, J. A. (2000). Heterogeneity of eukaryotic replicons, replicon clusters, and replication foci. *Chromosoma* **108**, 471-484.

Bleichert, F., Botchan, M. R. and Berger, J. M. (2015). Crystal structure of the eukaryotic origin recognition complex. *Nature* **519**, 321-326.

Blow, J. J., Dilworth, S. M., Dingwall, C., Mills, A. D. and Laskey, R. A. (1987). Chromosome replication in cell-free systems from Xenopus eggs. *Philos. Trans. R. Soc. Lond. B Biol. Sci.* **317**, 483-494.

Boria, I., Gruber, A. R., Tanzer, A., Bernhart, S. H., Lorenz, R., Mueller, M. M., Hofacker, I. L. and Stadler, P. F. (2010). Nematode sbRNAs: homologs of vertebrate Y RNAs. *J. Mol. Evol.* **70**, 346-358.

Christov, C. P., Gardiner, T. J., Szüts, D. and Krude, T. (2006). Functional requirement of noncoding Y RNAs for human chromosomal DNA replication. *Mol. Cell. Biol.* **26**, 6993-7004.

Christov, C. P., Trivier, E. and Krude, T. (2008). Noncoding human Y RNAs are overexpressed in tumours and required for cell proliferation. *Br. J. Cancer* **98**, 981-988.

Collart, C., Christov, C. P., Smith, J. C. and Krude, T. (2011). The midblastula transition defines the onset of Y RNA-dependent DNA replication in Xenopus laevis. *Mol. Cell. Biol.* **31**, 3857-3870.

Costa, A., Hood, I. V. and Berger, J. M. (2013). Mechanisms for initiating cellular DNA replication. *Annu. Rev. Biochem.* **82**, 25-54.

Fabini, G., Raijmakers, R., Hayer, S., Fouraux, M. A., Pruijn, G. J. M. and Steiner, G. (2001). The heterogeneous nuclear ribonucleoproteins I and K interact with a subset of the ro ribonucleoprotein-associated Y RNAs in vitro and in vivo. *J. Biol. Chem.* **276**, 20711-20718.

Farris, A. D., Puvion-Dutilleul, F., Puvion, E., Harley, J. B. and Lee, L. A. (1997). The ultrastructural localization of 60-kDa Ro protein and human cytoplasmic RNAs: association with novel electron-dense bodies. *Proc. Natl. Acad. Sci. USA* **94**, 3040-3045.

Fragkos, M., Ganier, O., Coulombe, P. and Méchali, M. (2015). DNA replication origin activation in space and time. *Nat. Rev. Mol. Cell Biol.* **16**, 360-374.

Gardiner, T. J., Christov, C. P., Langley, A. R. and Krude, T. (2009). A conserved motif of vertebrate Y RNAs essential for chromosomal DNA replication. *RNA* **15**, 1375-1385.

Gendron, M., Roberge, D. and Boire, G. (2001). Heterogeneity of human Ro ribonucleoproteins (RNPS): nuclear retention of Ro RNPS containing the human hY5 RNA in human and mouse cells. *Clin. Exp. Immunol.* **125**, 162-168.

Gerhardt, J., Jafar, S., Spindler, M.-P., Ott, E. and Schepers, A. (2006). Identification of new human origins of DNA replication by an origin-trapping assay. *Mol. Cell. Biol.* **26**, 7731-7746.

Ginisty, H., Sicard, H., Roger, B. and Bouvet, P. (1999). Structure and functions of nucleolin. *J. Cell Sci.* **112**, 761-772.

Hall, A. E., Turnbull, C. and Dalmay, T. (2013). Y RNAs: recent developments. *Biomol. Concepts* **4**, 103-110.

Hendrick, J. P., Wolin, S. L., Rinke, J., Lerner, M. R. and Steitz, J. A. (1981). Ro small cytoplasmic ribonucleoproteins are a subclass of La ribonucleoproteins: further characterization of the Ro and La small ribonucleoproteins from uninfected mammalian cells. *Mol. Cell. Biol.* **1**, 1138-1149.

Hogg, J. R. and Collins, K. (2007). Human Y5 RNA specializes a Ro ribonucleoprotein for 5S ribosomal RNA quality control. *Genes Dev.* **21**, 3067-3072.

Huberman, J. A. and Riggs, A. D. (1968). On the mechanism of DNA replication in mammalian chromosomes. *J. Mol. Biol.* **32**, 327-341.

Kowalski, M. P. and Krude, T. (2015). Functional roles of non-coding Y RNAs. *Int. J. Biochem. Cell Biol.* **66**, 20-29.

Kowalski, M. P., Baylis, H. A. and Krude, T. (2015). Non-coding stem-bulge RNAs are required for cell proliferation and embryonic development in C. elegans. *J. Cell Sci.* **128**, 2118-2129.

Krude, T. (1999). Mimosine arrests proliferating human cells before onset of DNA replication in a dose-dependent manner. *Exp. Cell Res.* **247**, 148-159.

Krude, T., Musahl, C., Laskey, R. A. and Knippers, R. (1996). Human replication proteins hCdc21, hCdc46 and P1Mcm3 bind chromatin uniformly before S-phase and are displaced locally during DNA replication. *J. Cell Sci.* **109**, 309-318.

Krude, T., Jackman, M., Pines, J. and Laskey, R. A. (1997). Cyclin/Cdk-dependent initiation of DNA replication in a human cell-free system. *Cell* **88**, 109-119.

Krude, T., Christov, C. P., Hyrien, O. and Marheineke, K. (2009). Y RNA functions at the initiation step of mammalian chromosomal DNA replication. *J. Cell Sci.* **122**, 2836-2845.

Langley, A. R., Chambers, H., Christov, C. P. and Krude, T. (2010). Ribonucleoprotein particles containing non-coding Y RNAs, Ro60, La and nucleolin are not required for Y RNA function in DNA replication. *PLoS ONE* **5**, e13673.

Langley, A. R., Graf, S., Smith, J. C. and Krude, T. (2016). Genome-wide identification and characterisation of human DNA replication origins by initiation site sequencing (ini-seq). *Nucleic Acids Res.* **44**, 10230-10247.

Laskey, R. A., Harland, R. M., Earnshaw, W. C. and Dingwall, C. (1981). Chromatin assembly and the co-ordination of DNA replication in the eukaryotic chromosome. In *International Cell Biology 1980-1981* (ed. H. G. Schweiger), pp. 162-167. Berlin: Springer Verlag.

Lerner, M. R., Boyle, J. A., Hardin, J. A. and Steitz, J. A. (1981). Two novel classes of small ribonucleoproteins detected by antibodies associated with lupus erythematosus. *Science* **211**, 400-402.

Matera, A. G., Frey, M. R., Margelot, K. and Wolin, S. L. (1995). A perinucleolar compartment contains several RNA polymerase III transcripts as well as the polypyrimidine tract-binding protein, hnRNP I. *J. Cell Biol.* **129**, 1181-1193.

Méndez, J., Zou-Yang, X. H., Kim, S.-Y., Hidaka, M., Tansey, W. P. and Stillman, B. (2002). Human origin recognition complex large subunit is degraded by ubiquitin-mediated proteolysis after initiation of DNA replication. *Mol. Cell* **9**, 481-491.

Mohammad, M. M., Donti, T. R., Sebastian Yakisich, J., Smith, A. G. and Kapler, G. M. (2007). Tetrahymena ORC contains a ribosomal RNA fragment that participates in rDNA origin recognition. *EMBO J.* **26**, 5048-5060.

Norseen, J., Thomae, A., Sridharan, V., Aiyar, A., Schepers, A. and Lieberman, P. M. (2008). RNA-dependent recruitment of the origin recognition complex. *EMBO J.* **27**, 3024-3035.

O'Brien, C. A., Margelot, K. and Wolin, S. L. (1993). Xenopus Ro ribonucleoproteins: members of an evolutionarily conserved class of cytoplasmic ribonucleoproteins. *Proc. Natl. Acad. Sci. USA* **90**, 7250-7254.

O'Donnell, M., Langston, L. Stillman, B. (2013). Principles and concepts of DNA replication in bacteria, archaea, and eukarya. *Cold Spring Harb. Perspect. Biol.* **5**, a010108.

Peek, R., Pruijn, G. J., van der Kemp, A. J. and van Venrooij, W. J. (1993). Subcellular distribution of Ro ribonucleoprotein complexes and their constituents. *J. Cell Sci.* **106**, 929-935.

Prasanth, S. G., Prasanth, K. V., Siddiqui, K., Spector, D. L. and Stillman, B. (2004). Human Orc2 localizes to centrosomes, centromeres and heterochromatin during chromosome inheritance. *EMBO J.* **23**, 2651-2663.

Pruijn, G. J., Simons, F. H. and van Venrooij, W. J. (1997). Intracellular localization and nucleocytoplasmic transport of Ro RNP components. *Eur. J. Cell Biol.* **74**, 123-132.

Siddiqui, K. and Stillman, B. (2007). ATP-dependent assembly of the human origin recognition complex. *J. Biol. Chem.* **282**, 32370-32383.

Siddiqui, K., On, K. F. and Diffley, J. F. (2013). Regulating DNA replication in eukarya. *Cold Spring Harb. Perspect. Biol.* **5**, a012930.

Simons, F. H., Pruijn, G. J. and van Venrooij, W. J. (1994). Analysis of the intracellular localization and assembly of Ro ribonucleoprotein particles by microinjection into Xenopus laevis oocytes. *J. Cell Biol.* **125**, 981-988.

Steitz, J. A., Berg, C., Hendrick, J. P., La Branche-Chabot, H., Metspalu, A., Rinke, J. and Yario, T. (1988). A 5S rRNA/L5 complex is a precursor to ribosome assembly in mammalian cells. *J. Cell Biol.* **106**, 545-556.

Tatsumi, Y., Ohta, S., Kimura, H., Tsurimoto, T. and Obuse, C. (2003). The ORC1 cycle in human cells: I. cell cycle-regulated oscillation of human ORC1. *J. Biol. Chem.* **278**, 41528-41534.

Teunissen, S. W. M., Kruithof, M. J., Farris, A. D., Harley, J. B., Venrooij, W. J. and Pruijn, G. J. (2000). Conserved features of Y RNAs: a comparison of experimentally derived secondary structures. *Nucleic Acids Res.* **28**, 610-619.

van Gelder, C. W. G., Thijssen, J. P. H. M., Klaassen, E. C. J., Sturchler, C., Krol, A., van Venrooij, W. J. and Pruijn, G. J. M. (1994). Common structural features of the Ro RNP associated hY1 and hY5 RNAs. *Nucleic Acids Res.* **22**, 2498-2506.

Wang, I., Kowalski, M. P., Langley, A. R., Rodriguez, R., Balasubramanian, S., Hsu, S.-T. D. and Krude, T. (2014). Nucleotide contributions to the structural integrity and DNA replication initiation activity of noncoding y RNA. *Biochemistry* **53**, 5848-5863.

Wolin, S. L. and Steitz, J. A. (1983). Genes for two small cytoplasmic Ro RNAs are adjacent and appear to be single-copy in the human genome. *Cell* **32**, 735-744.

Yeeles, J. T. P., Deegan, T. D., Janska, A., Early, A. and Diffley, J. F. X. (2015). Regulated eukaryotic DNA replication origin firing with purified proteins. *Nature* **519**, 431-435.

Zhang, A. T., Langley, A. R., Christov, C. P., Kheir, E., Shafee, T., Gardiner, T. J. and Krude, T. (2011). Dynamic interaction of Y RNAs with chromatin and initiation proteins during human DNA replication. *J. Cell Sci.* **124**, 2058-2069.